



Observed monsoon precipitation suppression caused by anomalous interhemispheric aerosol transport

Osinachi Ajoku¹ · Joel R. Norris¹ · Arthur J. Miller¹

Received: 1 March 2019 / Accepted: 3 November 2019 / Published online: 12 November 2019
© Springer-Verlag GmbH Germany, part of Springer Nature 2019

Abstract

This study uses observations and atmospheric reanalysis products in order to understand the impacts of smoke aerosols advected from the Southern Hemisphere on the dynamics of the West African monsoon. Seasonal biomass burning and resulting aerosol emissions have been well documented to affect regional weather patterns, especially low-level convection. Out of all monsoon months, precipitation shows the most variability over land during August, in which anomalous smoke aerosol values can increase (decrease) by 33% (29%) in the Northern Gulf of Guinea and precipitation can decrease (increase) by up to $\sim 2.5 \text{ mm day}^{-1}$ ($\sim 3 \text{ mm day}^{-1}$) along the West African monsoon region accounting for a 17% (18%) change in precipitation. Smoke aerosols produced by biomass burning occurring near Central Africa are advected towards the Gulf of Guinea at elevations around the 850 hPa level. Satellite observations show an increase (decrease) in cloud fraction and optical depth below (above) the 300-hPa level in the Gulf of Guinea and along the West African coastline along with concurrent decreases (increases) in cloud droplet radius during dirty (clean) aerosol episodes. Additional observations of shortwave radiation quantify changes in cloud coverage and monsoon dynamics. On average, reductions in surface shortwave radiation of $\sim 10\text{--}15 \text{ W m}^{-2}$ occur over the Gulf of Guinea during increased aerosol transport, with aerosols accounting for $\sim 33\text{--}50\%$ of that reduction. Reductions in shortwave radiation are associated with decreased convective available potential energy (CAPE). This demonstrates that increased transport of aerosols perturbs surface radiation, convection in the lower troposphere and eventually cloud coverage, potentially leading to the observed monsoon precipitation suppression. In a broader social context, this region houses 200 million people and thus understanding these climate patterns may carry great importance.

Keywords Biomass-burning · West African monsoon · Aerosols · Climate forcing

1 Introduction

Anthropogenic and natural combustion emissions, including biomass burning, are major sources of greenhouse gases such as nitrogen oxide and carbon dioxide, as well as aerosol particles. Aerosols, particulates in the atmosphere, have the potential to be transported more than 10,000 km downwind of emission sources (Clarke et al. 2001), where they can alter local radiation budgets and cloud formation

processes. Aerosols directly impact the planetary energy balance through the absorption and scattering of incoming radiation (Ramanathan et al. 2001; Haywood and Boucher 2000), which is known as the “direct effect”. Some aerosols act as cloud condensation nuclei (CCN), thereby influencing cloud droplet size and consequently the likelihood of coalescence and the accumulation of liquid water and ice in clouds, thus altering cloud albedo and lifetime (Twomey et al. 1987; Albrecht 1989; Ferek et al. 2000; Ghan et al. 2012). This is the so-called “indirect effect”. The direct and indirect effects caused by aerosols might induce changes in convection and precipitation patterns. The change in globally measured radiative forcing from the preindustrial to the present due to interactions between aerosol particles and cloud cover has the largest uncertainty of all anthropogenic factors (Stocker et al. 2013).

Carbonaceous aerosols in the atmosphere both scatter and absorb radiation. The absorbing component, generally

Electronic supplementary material The online version of this article (<https://doi.org/10.1007/s00382-019-05046-y>) contains supplementary material, which is available to authorized users.

✉ Osinachi Ajoku
oajoku@ucsd.edu

¹ Scripps Institution of Oceanography, University of California, San Diego, 9500 Gilman Dr., La Jolla, CA 92093, USA

referenced as black carbon (BC), is mainly soot produced from incomplete combustion. BC can absorb shortwave radiation efficiently and heat the atmosphere, thus leading to cloud dissipation if the aerosols are co-located with the clouds. This is the so-called “semi-direct effect”. The scattering component is generally referred to as organic carbon (OC) since these aerosols contain organic matter. It should be noted that BC also scatters radiation and although initially hydrophobic, becomes hydrophilic when aged and thus can act as CCN (Croft et al. 2005). Observations from Earth observing satellites indicate that carbonaceous aerosols are widespread with about 80% of biomass aerosols originating in the tropics (Dentener et al. 2006). Estimates of the magnitude of radiative forcing by carbonaceous aerosols carry considerable uncertainty. Radiative forcing by carbonaceous aerosols can alter surface solar radiation (Wild 2012) and the hydrological cycle (Ramanathan et al. 2001).

Uncertainties of aerosol emissions are large in the tropics, where 50% originate from anthropogenic fires. Smoke emissions from biomass burning account for 20% of the global sum of all aerosol emissions, but smoke emissions in tropical regions account for 12% of the global aerosol burden alone (Dentener et al. 2006; Marlon et al. 2008). Regions with substantial aerosol emissions from biomass burning suffer from frequent drought episodes and other disruptions to the hydrological cycle, with adverse societal impacts that have been widely reported during the last several decades. Africa is the single largest continental source of biomass burning emission and has a vast, complex terrain with stark contrast in geography, most notably the elevation and land cover transitions from southern to central Africa that aid the process of natural fires. African biomass burning peaks during local dry seasons, occurring near savannah-dominated land, and is thus geographically and temporally constrained by spatial and seasonal variations in precipitation. In the Northern Hemisphere, burning is confined between the Sahara Desert to the north and the Congo Rainforest to the south ($\sim 5^{\circ}\text{N}$ – 15°N), and in the Southern Hemisphere, burning is confined between the Kalahari Desert to the south and the rainforest towards the north ($\sim 10^{\circ}\text{S}$ – 15°S).

Previous studies have demonstrated links between carbonaceous aerosols and changes in local climate. Ramanathan et al. (2005) documented increases in atmospheric stability caused by the presence of BC and OC that significantly impact the intensity of Indian Monsoons. Modeling studies investigating aerosol effects on precipitation have been conducted over East Asia (Liu et al. 2011; Xie et al. 2016). Such aerosols have been shown to either invigorate or inhibit cloud formation (Koren et al. 2008) and may reinforce existing drought conditions (Rosenfeld et al. 2008; Zhang et al. 2009). Aerosol loading over West Africa during wet and dry seasons has been linked to correlations in wind intensity (Nwofor et al. 2018). Using direct satellite observations,

Tosca et al. (2015) found that a higher smoke burden limits upward vertical motion and increases surface pressure during the African fire season, indicative of convective suppression. A study by Huang et al. (2009a) utilized back trajectory and regression analysis to determine that both dust and smoke contribute to precipitation suppression over the West African monsoon (WAM) region; however, this study focused on the local dry season in which precipitation is minimal. More so, the mechanisms connecting aerosols and precipitation suppression are not well understood. The misrepresentation of black carbon aerosols across climate models creates uncertainty in our understanding of the mechanisms by which aerosols may impact regional climate. None of the abovementioned studies quantitatively show ways in which smoke aerosols impact the WAM region during the monsoon season.

Recent aerosol aircraft measurement campaigns have been conducted to analyze the potential impacts that smoke emissions from Central Africa have on clouds and precipitation in the tropical Atlantic. NASA’s Observations of Aerosols above Clouds and their Interactions (ORACLES; <https://espo.nasa.gov/oracles>) campaign sampled cloud and aerosol layers in the Southeast Atlantic between peak biomass burning season (Aug–Oct) for 2016–2018 to characterize seasonal offshore aerosol loading and aerosol-cloud interactions. The UK CLARIFY 2016 (Clouds and Aerosol Radiative Impacts and Forcing; Year 2016) campaign took similar samples at St. Helena Island (Zuidema et al. 2016). The Dynamic-Aerosol-Chemistry-Cloud-Interactions in West Africa (DACCIWA) project also took place in the summer of 2016 and involved a campaign near coastal West Africa. Here, the synoptic and mesoscale weather systems accompanying aerosol transport and monsoon dynamics are well documented (Knippertz et al. 2017).

In order to further understand the aerosol-associated changes in WAM dynamics, we examine possible linkages between biomass-burning aerosols and cloud formation and local radiation budgets. Bouniol et al. (2012, their Fig. 5) analyzed cloud frequency occurrence in a study region encompassing our own during the 2008 monsoon season using CloudSat radar and CALIPSO lidar. Tracing the path that aerosols follow from their source to the WAM, cloud types transition from stratocumulus over the GoG towards tall, cumulonimbus decks over the continent associated with the monsoon (Deetz et al. 2018). This cloud transition may be influenced by the presence of aerosol, so we correspondingly analyze potential impacts that aerosols may have on clouds of various types.

In this study, we show how anomalous aerosol transport may affect meteorological variables associated with monsoon precipitation, including cloud coverage as well as short-wave (SW) radiation budgets. Here, we document regions in Central Africa with maximum aerosol emissions

and follow their path across the equator and over the ocean towards the West African coastline. At this location, the potential effects that aerosol loading may have on cloud cover and radiative properties are analyzed. Unlike previous studies, this research focuses on aerosol-cloud-precipitation interactions during the local dry season over aerosol source regions and local monsoon season over impact regions covering a span of 13 years. Utilized datasets and descriptions of methodology are presented in the next section, followed by analyzed results and concluding remarks.

2 Datasets and methods

In order to determine how changes in aerosol loading over source regions impact monsoon precipitation downwind, daily-averaged or time-specific data (GMT) are utilized from a variety of sources (with the exception of fire emissions). Using daily intervals of data allows for a better sampling resolution as well as capturing mesoscale and synoptic-scale weather processes that would not be resolved with monthly data output.

Monthly fire carbon emissions (Giglio et al. 2013) are acquired from the Global Fire Emissions Database (GFED) at $0.25^\circ \times 0.25^\circ$ resolution. These data include burn area resulting from small fires and are used only to understand seasonal changes in fire distribution throughout the continent (Van Der Werf et al. 2017).

Daily aerosol optical depth (AOD) for the years 2003–2015 are obtained from Modern-Era Retrospective analysis for Research and Applications, Version 2 (MERRA-2) at $0.5^\circ \times 0.625^\circ$ resolution (GMAO 2015). The reason for selecting this time period is that it coincides with the launch of the Aqua mission that provides purely observed data onboard NASA's A-train constellation. Like most satellite observations, data are not available for areas outside the satellite swath path. Having missing AOD data can lead to large errors when undergoing statistical analysis. Using reanalysis data reduces such errors as data not captured by observations are assimilated using a numerical algorithm to create a synthesized estimate of the state of the climate system (Bengtsson et al. 2004). Observations, such as the aerosol index and aerosol absorption optical depth obtained from the Ozone Monitoring Instrument (OMI) measurements and aerosol retrievals from the AEROSOL ROBOTIC NETWORK (AERONET) (Buchard et al. 2015) validated the data obtained from reanalysis used in our study. We note that this study claims that AOD values in Southern Africa biomass burning regions from MERRA are underestimated.

In order to quantify the magnitude and location of anomalous changes in rainfall, daily data at 1-degree resolution is obtained from the Global Precipitation Climatology Project, Version 1.2 (GPCP 1.2). All the GPCP products

are produced by optimally merging precipitation estimates computed from microwave, infrared, sounder data observed on board satellites, and ground-based rain gauge analysis, taking advantage of the strengths of each data type (Huffman et al. 2016). These satellite datasets have been validated against rain gauges on land in West Africa, particularly on sub-monthly time scales (Nicholson et al. 2003).

Daily wind fields (zonal, meridional and vertical), temperature, specific humidity, convective available potential energy (CAPE), sea level pressure and geopotential height data at 0.75° by 0.75° resolution were obtained at multiple pressure levels ranging from the surface to 500 hPa from the European Centre for Medium-Range Weather Forecasts (ECMWF) reanalysis product (Berrisford et al. 2011) at a local time of 6 A.M. UTC, which is consistent with the analysis of Tosca et al. (2015). Here, they studied the changes in cloud fraction associated with variability in fire emissions and compared meteorological variables in control and high fire scenes using ECMWF reanalysis at a 6 am local time to better understand the influence of mesoscale dynamics. Furthermore, mid-level clouds have been found to dominate cover over West Africa during the monsoon season early in the morning (Bourgeois et al. 2018).

To analyze the effect of aerosols on cloud cover, we obtained computed, surface radiation fluxes and cloud coverage during the study period from Clouds and the Earth's Radiant Energy System (CERES) data, which is available, daily-averaged, at 1-degree resolution (Doelling et al. 2013, 2016). This data is broken down into 4 vertical cloud levels (low, mid-low, mid-high and high). Cloud properties are determined using simultaneous measurements by other EOS and S-NPP instruments such as the Moderate Resolution Imaging Spectroradiometer (MODIS) and the Visible and Infrared Sounder (VIRS). We calculate aerosol forcings by subtracting surface fluxes from computed surface fluxes with aerosols removed in order to gain a better understanding for local radiation budgets. Their computed fluxes are produced using the Langley Fu–Liou radiative transfer model. Here, observed aerosol values are obtained using MODIS and computations are constrained to the observed CERES TOA fluxes.

Our study regions in the northern Gulf of Guinea (GoG) and WAM comprise of the boundaries between 0° – 5° N and 10° W– 10° E and 5° N– 10° N and 10° W– 10° E respectively. For each of the 13 years, the 31 days in August were classified into pentiles according to the magnitude of AOD averaged over the study region in the GoG for that day. This pentile sampling is done independently for each month in order to sample many different independent background meteorological states over the entire dataset (Results using the absolute dirtiest and cleanest days are very similar). The top and bottom pentiles each had 78 days and are referred to as “clean” (lowest AOD) and “dirty” (highest AOD) days.

All dates associated with these dirty and clean days are averaged together to create composites that track how aerosol loading evolves with other meteorological variables of interest. Climatological means are subtracted from composited data to reveal anomalous changes. By utilizing this method, we attempt to determine which variables control or are impacted by variations in aerosol transport. Statistical significance of results was determined by the 95% confidence interval according to a 2-tailed Student's t test accounting for serial correlation by using the effective sample size, $n(1 - r_1)(1 + r_1)^{-1}$, where n is the number of days and r_1 is the lag-1 autocorrelation coefficient leading to ~ 3 day decorrelation time.

3 Results

3.1 Climatology

African biomass burning peaks during local dry seasons, occurring where tropical rainforests transition into savannah-dominated lands, and is thus geographically constrained by seasonal variations in precipitation. For the current study, maximum aerosol emissions located in this transition zone occur during boreal summer/austral winter (regional dry season in the Southern Hemisphere). Figure 1 shows climatological carbon emissions associated with biomass burning over the period 2003–2015 for the month of August.

The WAM is distinguished by a northward migration of the Intertropical Convergence Zone (ITCZ) and a spatial shift in monsoon onset. Although the WAM occurs during June–September, the present study focuses on August because precipitation variability is largest over land relative to other months. During August, intense precipitation is present in Southern West Africa (Fig. 2). Figure 2 shows 925 hPa wind and precipitation climatology for the month of August. The West African westerly jet (WAWJ) is clearly evident at this pressure level (925 hPa) in the areas of deep convection near 8° – 11° N. This jet is responsible for transporting low-level moisture from the GoG toward land and is located at the ~ 900 hPa level throughout our study region.

Further south, winds from emission regions can be seen leading into the monsoon flow, which has been documented by reconstruction of the mean meridional circulation over West Africa and the GoG (Hourdin et al. 2010). Figure 3 shows the distribution of aerosol optical depth (AOD), a variable that measures the extinction of incoming solar radiation by airborne particulate matter over the African continent for August averaged during a 13-year observational record. Overlain on top of AOD are climatological winds averaged at 850 hPa over the same time period to give an idea as to where smoke aerosols are transported. Winds at this pressure level are used because they represent the conditions immediately above the planetary boundary level (PBL) and have been used in previous studies linking aerosols and precipitation near this region (Huang et al. 2009b; Wilcox

Fig. 1 Climatological August Biomass Burning Emissions for the years 2003–2015. Units are grams of Carbon $\text{m}^{-2} \text{month}^{-1}$

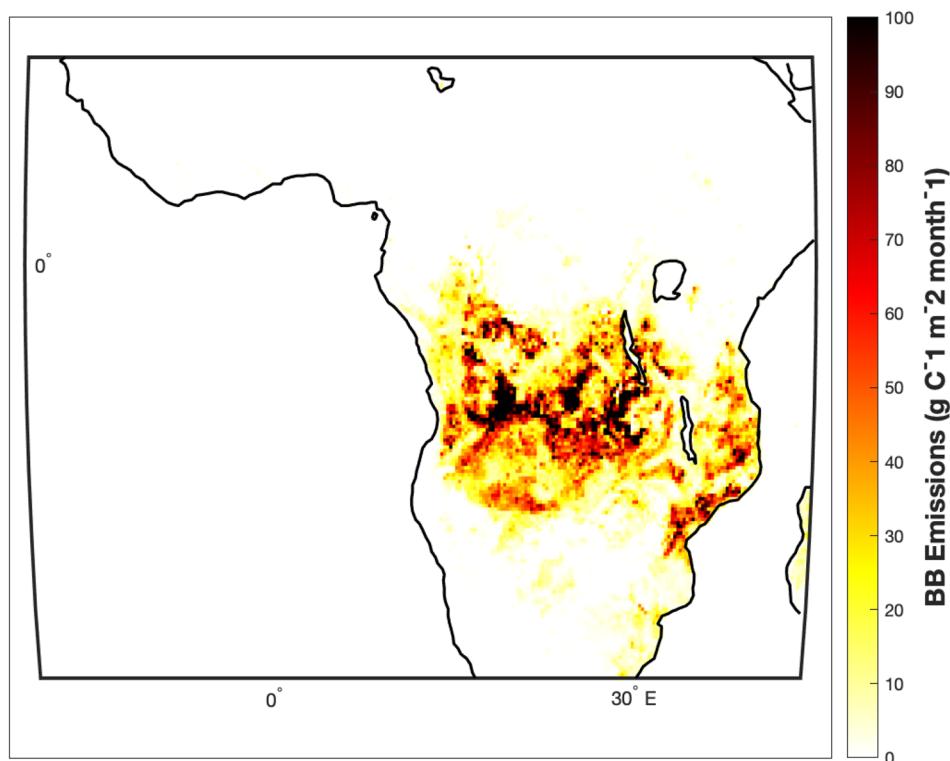


Fig. 2 925 hPa wind and precipitation climatology for the month of August. The box region reflects where precipitation analyses are carried out in subsequent figures

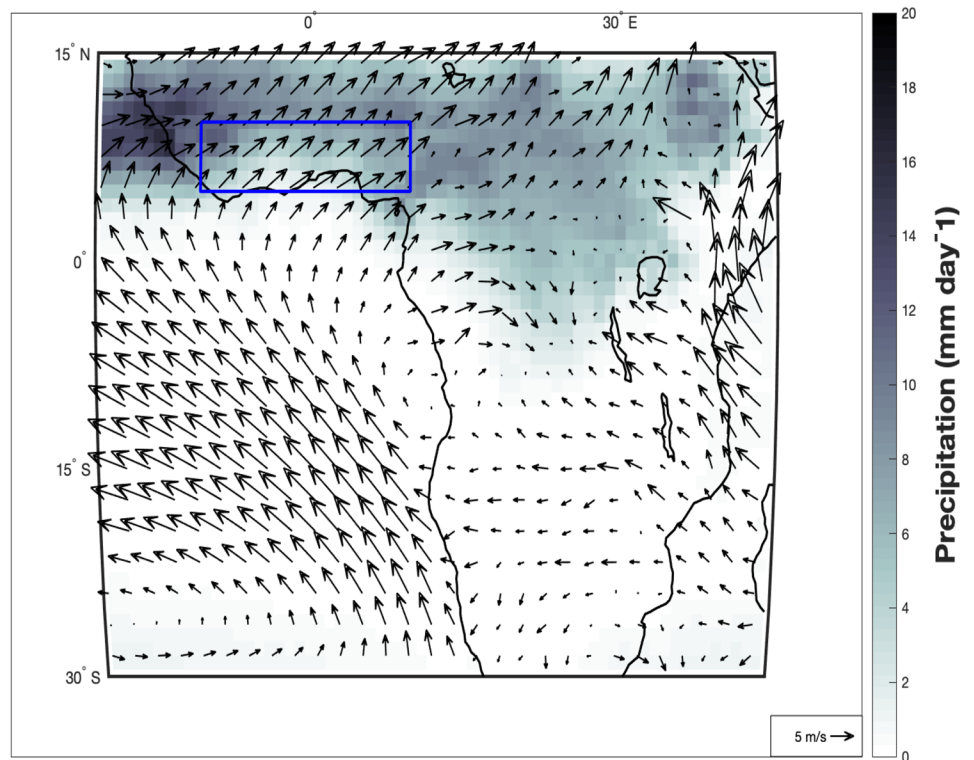
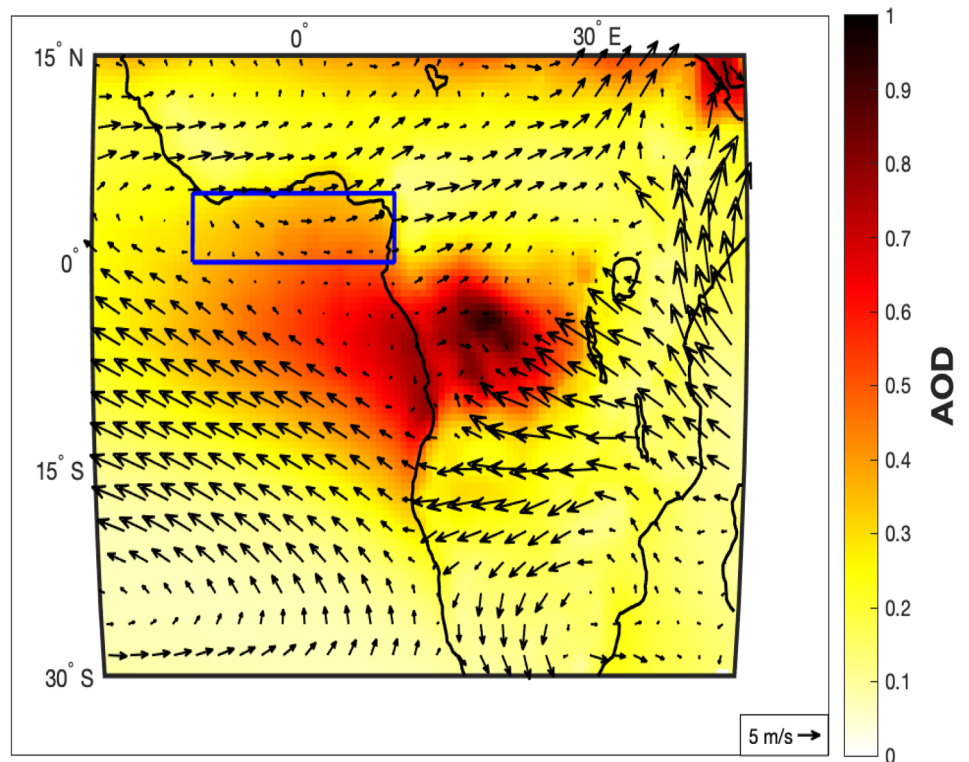


Fig. 3 850 hPa wind and column-integrated AOD climatology for the month of August. The box region reflects where AOD composites are created for analyses carried out in this study



et al. 2016). The GoG region is of particular focus because it is adjacent to both the source of aerosol emissions and areas impacted by the WAM.

3.2 Aerosol-cloud-SW radiation feedback in the WAM region

Figure 4 displays the composite anomalies in AOD and 850 hPa winds for dirty (top) and clean (bottom) days. Stippling represents AOD data that is significant at the 5% level, a convention that will be used for data in subsequent figures. It is clearly evident that anomalous transport of aerosols from Central Africa towards the GoG is caused by changes in wind direction and intensity over the source region. Coupled with Africa's complex topography, there exists anomalously higher/lower sea level pressures in Southern Africa that may impact the westward offshore transport of smoke (Adebisi et al. 2015; Kruger et al. 2010) and these factors lead towards observed, increased aerosol transport (Supplementary Fig. 1). Within the GoG, AOD values are, on average, $\sim 0.12 \pm 0.018$ higher than the climatological value of ~ 0.36 during episodes of increased transport, accounting for a 33% increase in aerosol presence. In contrast, AOD values are, on average, $\sim 0.11 \pm 0.011$ lower during episodes of decreased transport, accounting for a 29% decrease in aerosol presence. We refrain from conducting AOD analysis

over the WAM region to avoid possible aerosol washout by climatological precipitation.

The presence of increased (decreased) biomass burning aerosols is associated with slight increases (decreases) between ~ 2 and 4% in low-level cloud (surface–700 hPa) fraction over our study region in the GoG and Central African interior where aerosols are being transported from (Fig. 5). Considering that the GoG is predominantly covered with lower-level clouds, our results are consistent with Wilcox (2012) and Brioude et al. (2009), who analyzed observations that show that atmospheric warming due to solar absorption by biomass burning aerosols above the cloud layer may enhance the buoyancy of free-tropospheric air above the cloud, inhibit cloud top entrainment and lead to additional cloud thickening in the boundary layer. This may be potentially caused by the semi-direct aerosol effect.

Assuming that aerosols are initially transported around the 850 hPa height, aerosol impacts on higher level clouds would be a result of aerosol indirect effects. Therefore, we examine changes in cloud optical depth and cloud water radius (when adequate data is available) in addition to cloud fraction. Looking at mid-low cloud fraction anomalies (700–500 hPa), we find increases (decreases) up to 5% for dirty (clean) days respectively between the GoG and the West African coastal region (Figs. 6a and 7a). With an increase in aerosol amount at this particular level, there also

Fig. 4 AOD and 850 hPa wind anomalies for dirty (a) and clean (b) days for the month of August. Stippling represents AOD data that is significant at the 5% level

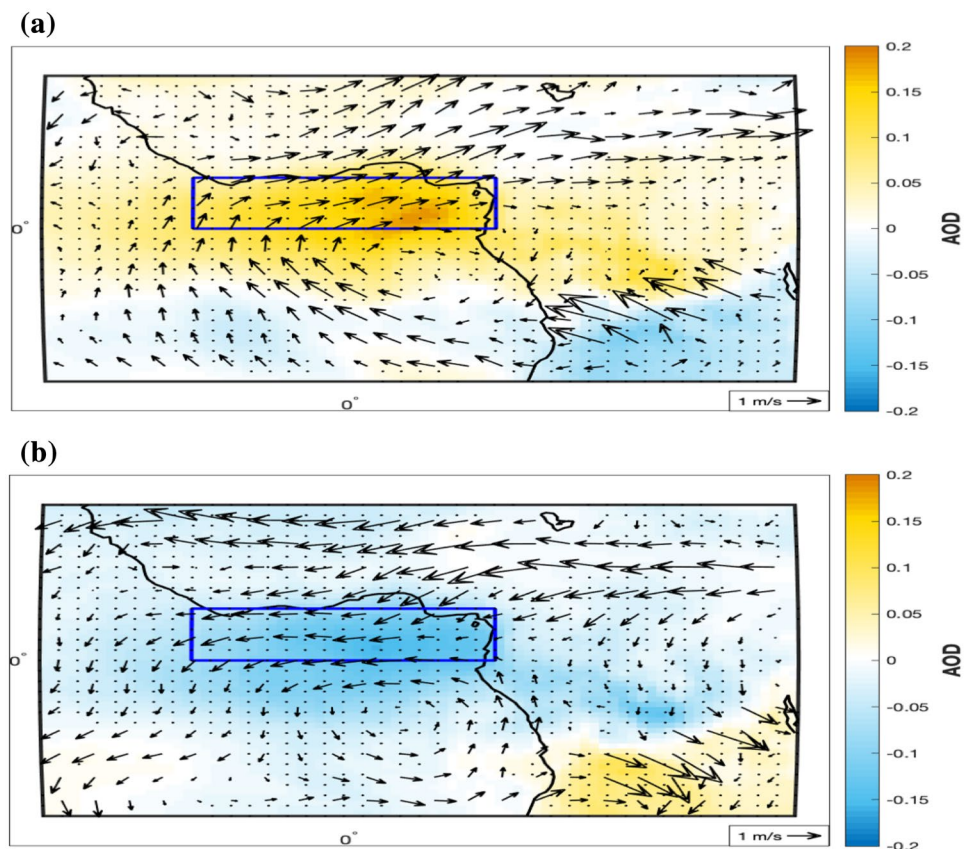
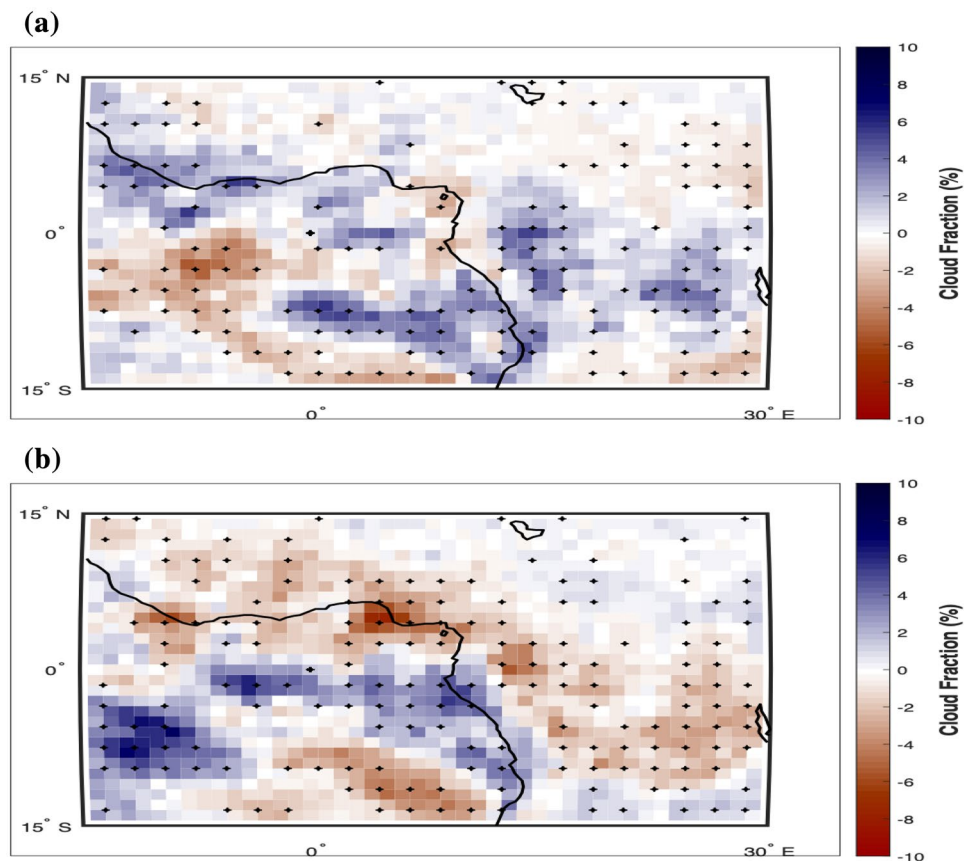


Fig. 5 Low-level cloud fraction (surface–700 hPa) anomalies during dirty **(a)** and clean **(b)** days for the month of August. Stippling represents data that is significant at the 5% level



exist increases in cloud optical depth (Fig. 6b). Our findings here are in agreement with Kaufman et al. (2005) who they find evidence of a smoke aerosol-induced indirect effect over the eastern Atlantic Ocean during monsoon months for both stratiform and cumulus cloud decks. They attribute increased low-level cloud fraction to dry air entrainment as well. We can see this signal clearly in the GoG on dirty days. The authors correlate increases in cloud coverage and aerosol loading at 3 km with decreases in cloud droplet effective radius (Fig. 6c). They also find similar results for cumulus clouds that penetrate through the smoke layer. Haywood et al. (2003) found that aerosols over the ocean have a clear separation from the underlying stratiform clouds, whereas over land, biomass-burning aerosols become well mixed up to 500 hPa. Over continental air, where deep convection is much stronger than over the ocean, aerosols are lofted into high-level, monsoon strength clouds. For middle high-level clouds (500–300 hPa), we find the highest increases in cloud fraction and optical depth over GoG and Southern West Africa (Fig. 8). Contrasting results are found for clean conditions (Fig. 9).

Changes in the number of absorbing aerosols and cloud fraction lead to further changes in surface heating, which is investigated further by analyzing SW radiation fluxes. Figure 10 shows CERES computed surface SW anomalies

during dirty days for the month of August, with the top (bottom) panel represents all-sky (aerosol-only) conditions. At the surface, we find reductions around $10\text{--}15\text{ W m}^{-2}$ for all-sky conditions that consist of both clear and cloudy skies, for which $\sim 5\text{ W m}^{-2}$ are due to the direct presence of aerosols. We also find contrasting results for clean days (Fig. 11). A reduction in surface shortwave radiation can decrease surface evaporation and energy available for convection. Therefore, we also explore changes in convective available potential energy (CAPE) during dirty and clean episodes (Fig. 12). When more (less) aerosols are present, a reduction (increase) in CAPE can be seen over our WAM land box and Central Africa where the bulk of monsoon-related precipitation occurs. CAPE reflects the potential vertical speed within an updraft and can be expected to impact the formation of clouds, especially towering cumulonimbus that reach the tropopause like our current study region. Composite temperature soundings over GoG reveal very little instability (Supplementary Fig. 2). To complete our analysis of a possible aerosol-cloud-SW radiation feedback, we include changes in high-level (300 hPa-tropopause) clouds (Fig. 13). On dirty days, we find reductions in high-level cloud fraction, which is in agreement our previous results showing decreases in surface SW radiation and reduced CAPE. Contrasting results are found on clean days as well.

Fig. 6 Changes in mid-low (700–500 hPa) cloud fraction (a), cloud optical depth (b) and cloud droplet radius in units of microns (c) for polluted aerosol conditions. Stippling represents cloud data that is significant at the 5% level

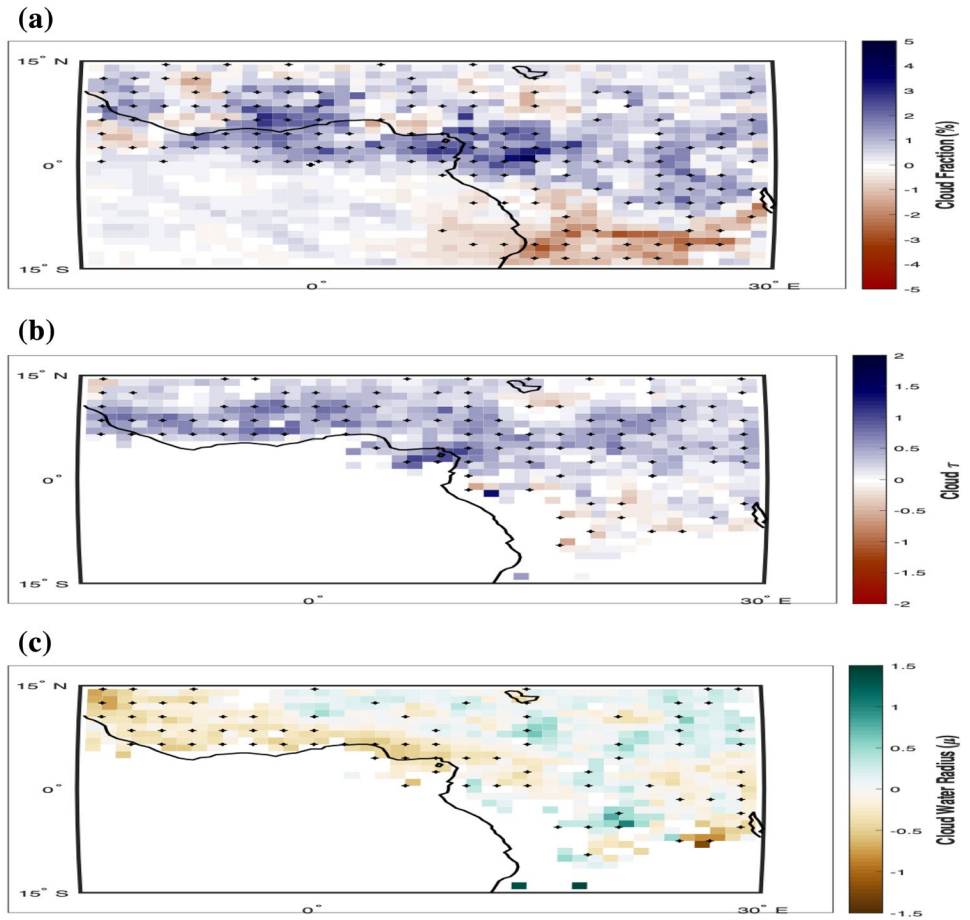


Fig. 7 Same as Fig. 6 but under clean aerosol conditions

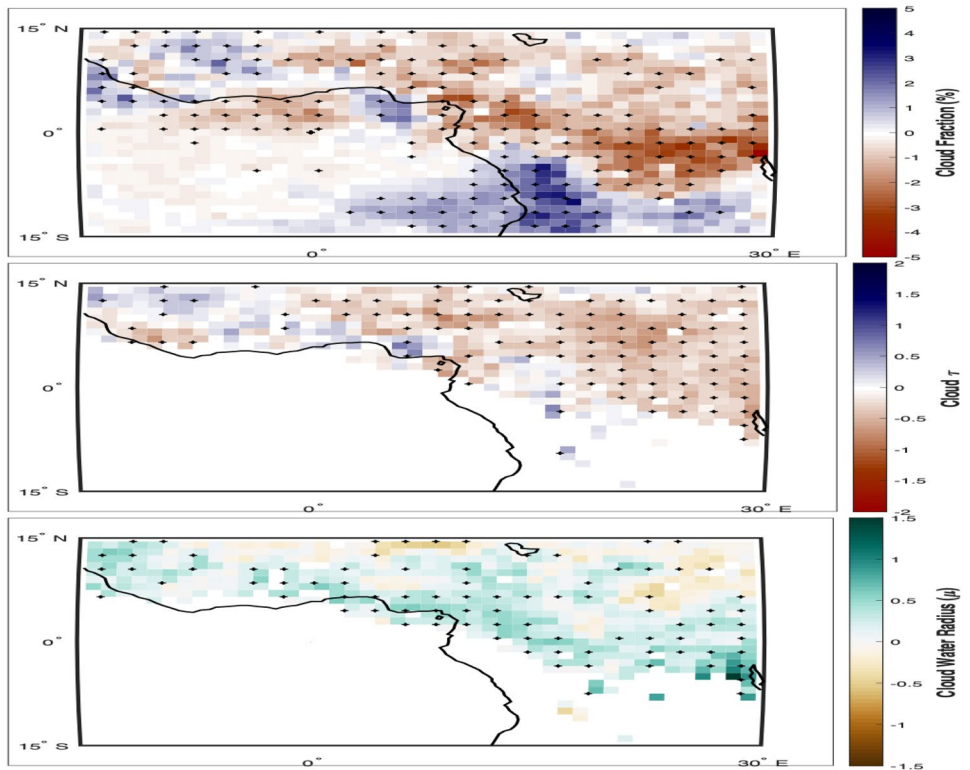


Fig. 8 Changes in mid-high (500–300 hPa) cloud fraction (a) and cloud optical depth (b) during polluted aerosol conditions. Stippling represents cloud data that is significant at the 5% level

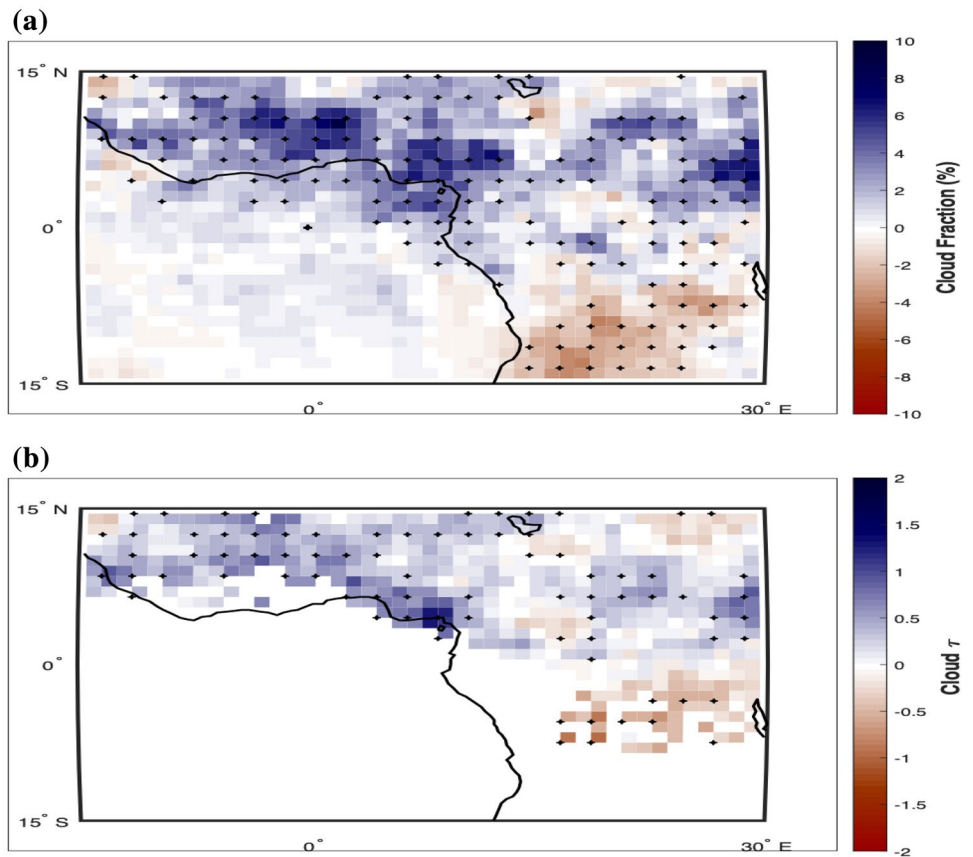


Fig. 9 Same as Fig. 8 but under clean aerosol conditions

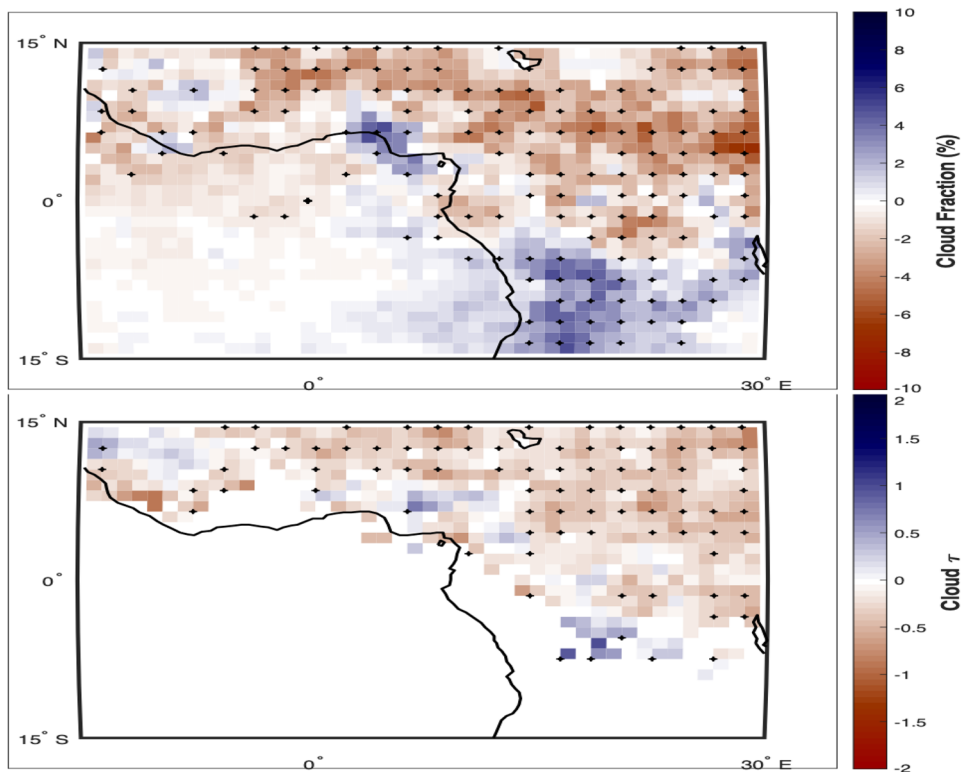


Fig. 10 CERES computed surface SW anomalies during dirty days for the month of August for all-sky (a) and aerosol-only (b) conditions for polluted days. Stippling represents data that is significant at the 5% level

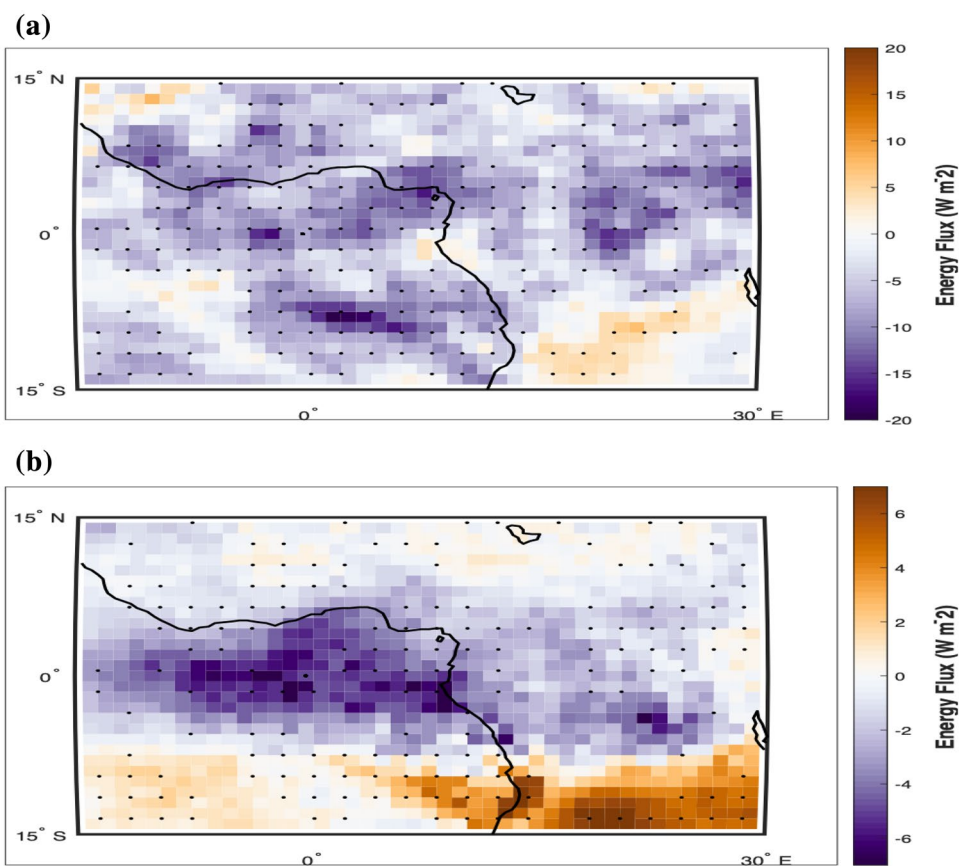


Fig. 11 Same as Fig. 10, but with clean days shown

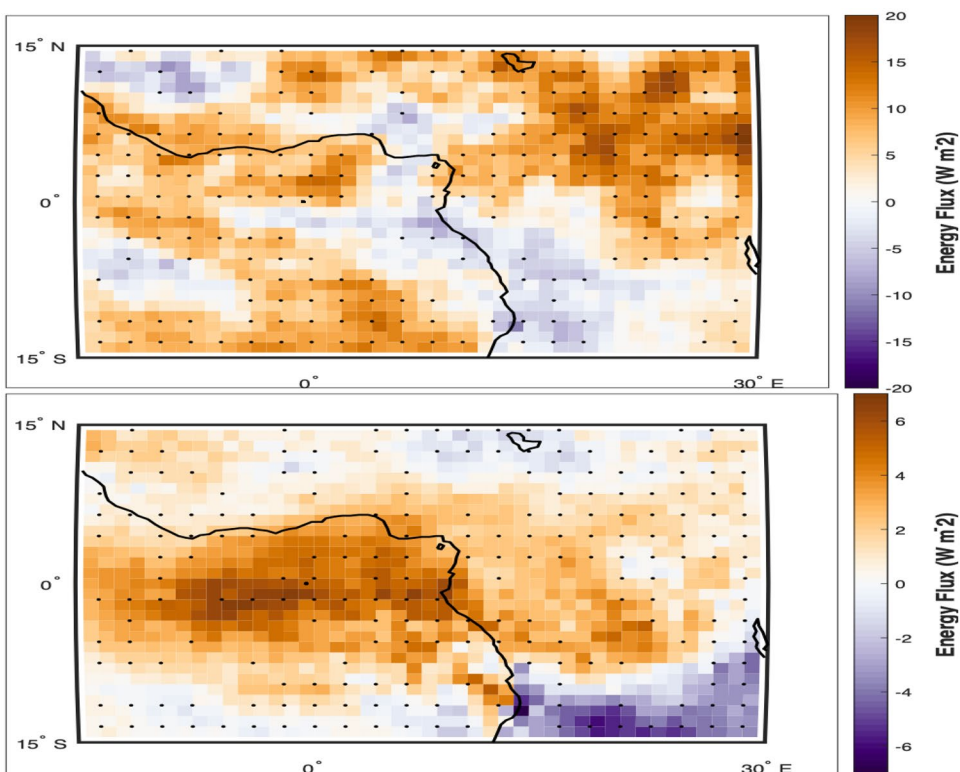
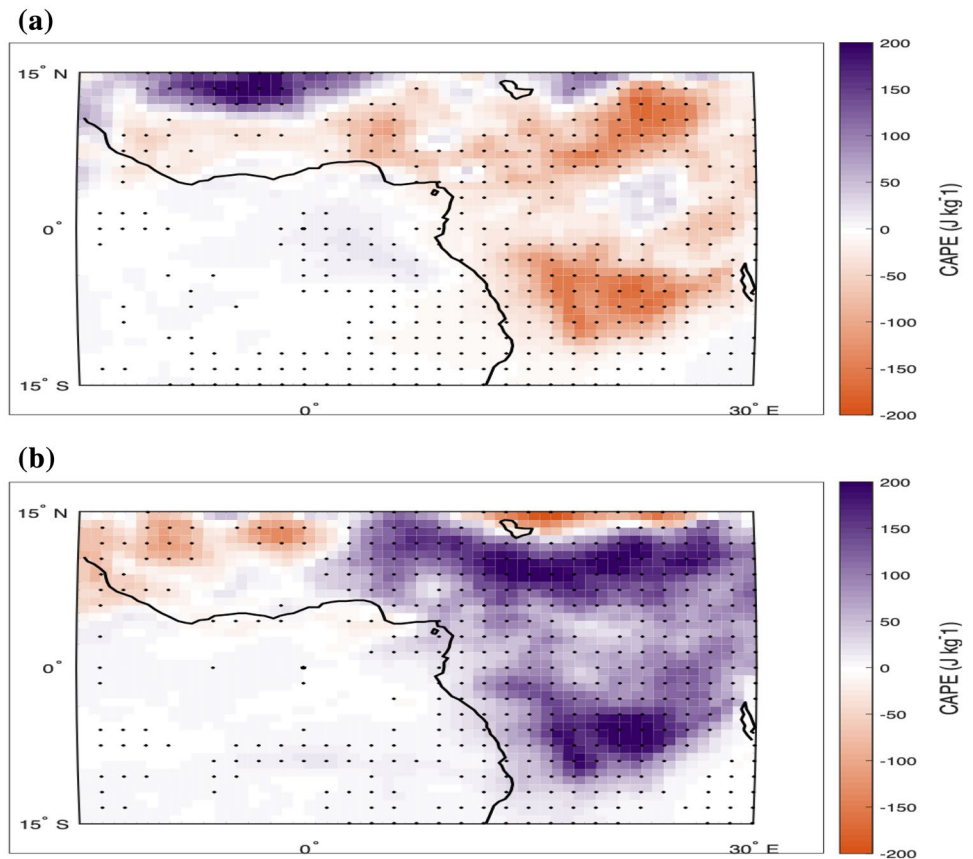


Fig. 12 Convective available potential energy (CAPE) anomalies for dirty (a) and clean (b) days in the month of August. Stippling represents data that is significant at the 5% level



3.3 Statistical relationships between anomalous aerosol transport and the WAM

These AOD, cloud and radiation anomalies within in the GoG, in turn, may potentially impact precipitation in the WAM region. Figure 14 shows precipitation and 925 hPa wind anomalies for dirty (top) and clean (bottom) days. Coinciding with dirty days over the GoG is an adjacent decrease in daily precipitation rates along the West African coastline towards its Sub-Saharan interior (Fig. 14, box region over West Africa). Decreases of 17% ($0.83 \text{ mm day}^{-1} \pm 0.75 \text{ mm day}^{-1}$ on average) relative to a 5.9 mm day^{-1} climatological value can be seen over densely populated countries like Nigeria whose agricultural sector relies on monsoonal rain for annual crop yields. In contrast, increases of 18% ($0.91 \text{ mm day}^{-1} \pm 0.8 \text{ mm day}^{-1}$ on average) are associated with clean days over the GoG.

For further analysis, we compared AOD and precipitation anomalies directly for the month of August during all study years comprising of 403 days by calculating box averages for each day. We use our aforementioned region in the GoG for AOD values, and a region spanning 4.5°N – 9.5°N and 9.5°E – 9.5°W for precipitation. This boundary encompasses the portion of West Africa that is directly adjacent of the GoG. Figure 15 displays a scatterplot comparing AOD and

precipitation rates, providing a good way to visualize how these two variables change together. This fit represents a statistically significant negative relationship and filled circles display where clean and dirty days fall amongst the August spread. For additional context, mean values for each variable are plotted in dotted lines. Previous investigations of relationships between aerosols and precipitation during the Indian summer monsoon are consistent with our results in that increased aerosol is associated with decreased precipitation (Ramanathan et al. 2005; Shindell et al. 2012).

A potential explanation for the observed precipitation reduction could be simply meteorological variability. What if changes in wind strength, specifically the meridional component can explain the precipitation variability in the WAM region? Ideally, stronger winds from the Gulf of Guinea are indicative of a stronger monsoon flow. If so, the previous connection between aerosols, precipitation, clouds and surface radiation fluxes is merely correlative and not causal. Looking closely at Fig. 14 shows stronger meridional winds (925 hPa) during dirty days, which would suggest a stronger jet and increased moisture transport, yet there is not an increase in precipitation. Thus, providing good reasoning that local meteorological variability cannot explain changes in aerosol amounts.

Fig. 13 High-level cloud fraction (300 hPa-tropopause) anomalies during dirty (a) and clean (b) days for the month of August. Stippling represents data that is significant at the 5% level

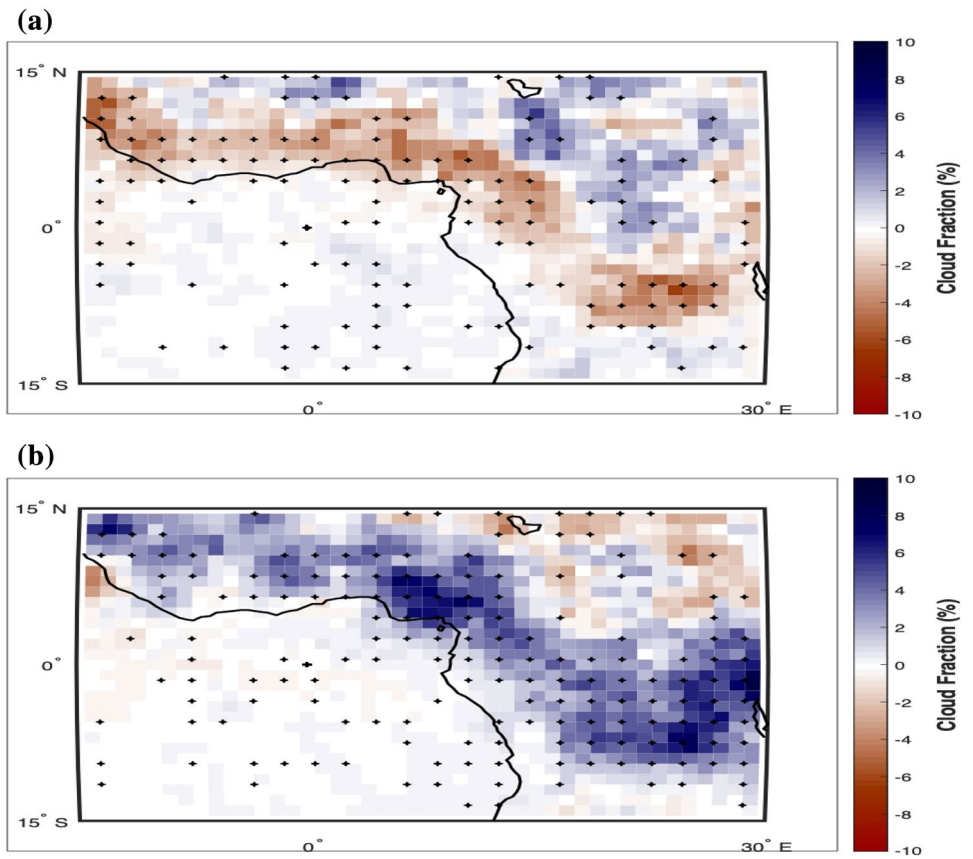


Fig. 14 Precipitation and 925 hPa wind anomalies for dirty (a) and clean (b) days for the month of August. Data significant at the 5% level is shown with filled, green circles. The blue box represents a region downwind of the GoG box highlighting precipitation anomalies

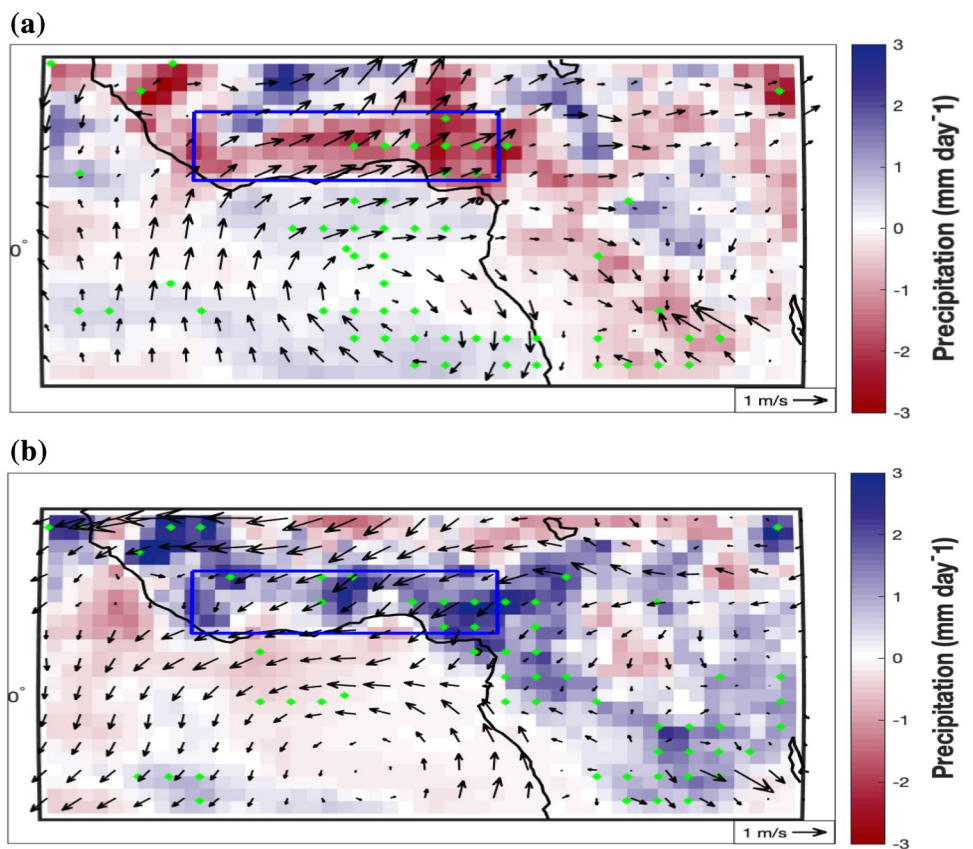
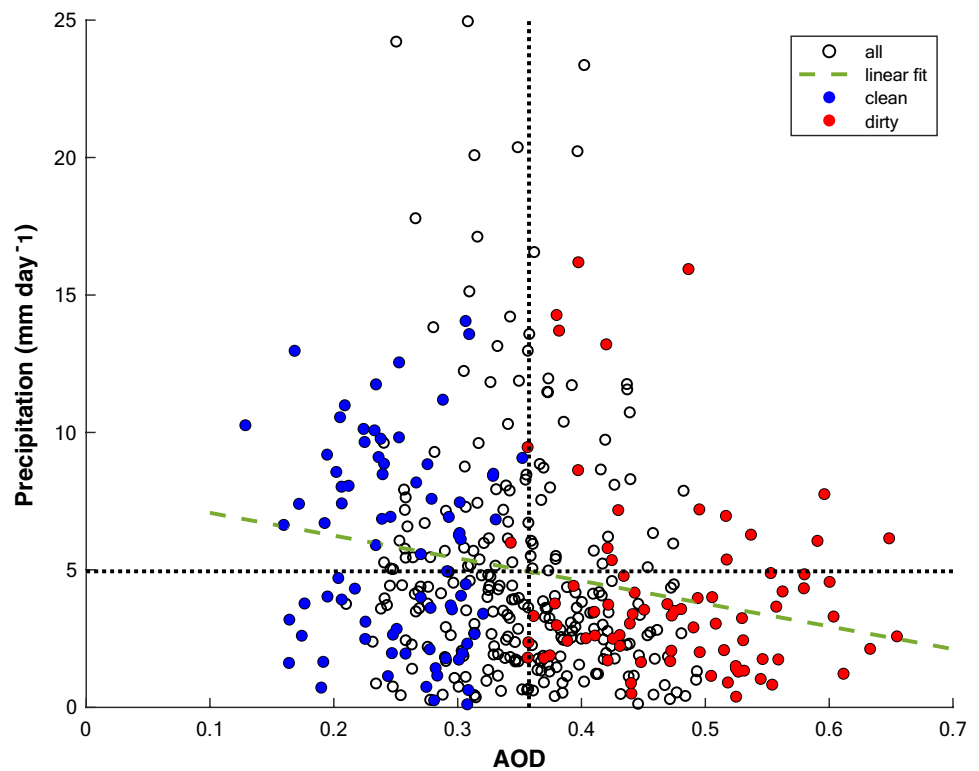


Fig. 15 Scatterplot of AOD over the Gulf of Guinea study region and precipitation over adjacent land in West Africa for the month of August. Precipitation values are obtained from averaging values in the box shown in Fig. 14. The red line represents a linear fit of this relationship and dotted circles are mean values for AOD and precipitation. Filled circles reflect data counted during dirty and clean aerosol days



4 Conclusion

Variations in wind intensity over source regions of smoke aerosols in tropical Africa leads to anomalous aerosol advection towards the GoG. During the peak in the local monsoon season, we found evidence linking increased aerosol presence with a reduction in precipitation over West Africa. To further understand the possible mechanisms by which this occurs, we analyzed other meteorological variables associated with precipitation.

First, we looked at changes in low level cloud properties associated with dirty and clean aerosol conditions. Throughout our study regions, fine-mode smoke aerosols (Adebiyi et al. 2015) interact with various cloud types and have two different effects on cloud coverage. A previous study using monthly CALIPSO observations indicated that the peak of smoke aerosols is about 650 hPa, which is well above the atmospheric boundary layer (Fig. 1b of Adebiyi and Zuidema 2018). There is evidence of a semi-direct radiative forcing caused by smoke aerosols in the GoG where low-level clouds dominate the region. At this location, low-level stratocumulus clouds can reside at a lower altitude than smoke aerosols coming from the continent possibly leading to additional cloud coverage. This proposed mechanism for a semi-direct radiative forcing is consistent with the results obtained by Wilcox (2012). Over land, where deep convection is more prevalent, we find evidence for the aerosol indirect effect. Near the West African coastline and Central

African interior, we observed increases in mid-level cloud formations during dirty days as shown in Fig. 8. Coupled with an increase in cloud fraction, we find corresponding increases in cloud thickness and decreases in cloud droplet radius. As elegantly noted by Koren et al. (2008), initial cloud fraction plays a critically important role in determining the balance between the two effects. This study further introduces two equations (Eqs. 4–5) representing aerosol direct/indirect effects and its contribution on total cloud fraction by superimposing these two equations (Koren et al. 2008, figure 1). Cloud fields with large cloud fraction will be affected mostly by microphysics, whereas fields with small cloud fraction will be inhibited by aerosol absorption since larger amounts of cloud free sky will be available for aerosol radiative effects to dominate.

The signal for elevated aerosol transport and increased low to mid-level cloud fraction shows itself in the surface SW flux, in which aerosols account for ~33% of the reduction in energy reaching the surface during dirty conditions. With the reduction in SW radiation reaching the surface, we see a corresponding decrease in CAPE which probably promotes a decrease in high-level cloud fraction. We suggest that aerosol radiative effects alter local radiation budgets, ultimately weakening the energy available for convection and reducing precipitation rates for the month of August in the WAM region.

While this paper proposes a mechanism by which smoke aerosols potentially inhibit monsoon driven precipitation

over West Africa, it remains necessary to evaluate how full-physics climate models simulate these aerosol-cloud-precipitation responses over this region, including which aerosol radiative effect is more dominant. Since this research takes a unique approach in linking connections between transport of biomass burning produced aerosols from a source region and monsoon precipitation in another region, there are few related studies for comparison. Additional research will help to clarify the mechanisms and potentially confirm the proposed interactive processes.

Acknowledgements This research forms a part of the Ph.D. dissertation of OA, who was supported by a National Science Foundation Graduate Research Fellowship (DGE-1650112) and a San Diego Foundation Fellowship. The National Science Foundation Earth System Modeling Program (OCE1419306) provided additional funding that supported this research. We thank Eric Wilcox, Andi Andreae, Amato Evan and Victor Dike for important discussions and suggestions. We also thank the three referees who provided very important comments that significantly improved our analysis and enhanced the clarity of our results.

References

- Adebiyi AA, Zuidema P (2018) Low cloud cover sensitivity to biomass-burning aerosols and meteorology over the southeast Atlantic. *J Clim* 31(11):4329–4346
- Adebiyi AA, Zuidema P, Abel SJ (2015) The convection of dynamics and moisture with the presence of shortwave absorbing aerosols over the southeast Atlantic. *J Clim* 28(5):1997–2024
- Albrecht B (1989) Aerosols, cloud microphysics, and fractional cloudiness. *Science* 245:1227–1230. <https://doi.org/10.1126/science.245.4923.1227>
- Bengtsson L, Hagemann S, Hodges KI (2004) Can climate trends be calculated from reanalysis data? *J Geophys Res Atmos* 109:D11111
- Berrisford P, Dee D, Poli P, Brugge R, Fielding K, Fuentes M, Simmonds A (2011) The ERA- Interim archive, version 2.0
- Bouniol D, Couvreux F, Kamsu-Tamo PH, Leplay M, Guichard F, Favot F, O'Connor EJ (2012) Diurnal and seasonal cycles of cloud occurrences, types, and radiative impact over West Africa. *J Appl Meteorol Climatol* 51(3):534–553
- Bourgeois E, Bouniol D, Couvreux F, Guichard F, Marsham JH, Garcia-Carreras L, Parker DJ (2018) Characteristics of mid-level clouds over West Africa. *Q J R Meteorol Soc* 144(711):426–442
- Brioude J, Cooper OR, Feingold G, Trainer M, Freitas SR, Kowal D, Frost GJ (2009) Effect of biomass burning on marine stratocumulus clouds off the California coast. *Atmos Chem Phys* 9(22):8841–8856
- Buchard V, da Silva AM, Colarco PR, Darmenov A, Randles CA, Govindaraju R, Spurr R (2015) Using the OMI aerosol index and absorption aerosol optical depth to evaluate the NASA MERRA Aerosol Reanalysis. *Atmos Chem Phys* 15(10):5743
- Clarke AD, Collins WG, Rasch PJ, Kapustin VN, Moore K, Howell S, Fuelberg HE (2001) Dust and pollution transport on global scales: aerosol measurements and model predictions. *J Geophys Res Atmos* 106(D23):32555–32569
- Croft B, Lohmann U, Salzen KV (2005) Black carbon ageing in the Canadian Centre for Climate modelling and analysis atmospheric general circulation model. *Atmos Chem Phys* 5(7):1931–1949
- Deetz K, Vogel H, Knippertz P, Adler B, Taylor J, Coe H, Bower K, Haslett S, Flynn M, Dorsey J, Crawford I, Kottmeier C, Vogel B (2018) Numerical simulations of aerosol radiative effects and their impact on clouds and atmospheric dynamics over southern West Africa. *Atmos Chem Phys* 18:9767–9788
- Dentener F, Kinne S, Bond T, Boucher O, Cofala J, Generoso S, Marelli L (2006) Emissions of primary aerosol and precursor gases in the years 2000 and 1750 prescribed data-sets for AeroCom. *Atmos Chem Phys* 6(12):4321–4344
- Doelling DR, Loeb NG, Keyes DF, Nordeen ML, Morstad D, Nguyen C, Sun M (2013) Geostationary enhanced temporal interpolation for CERES flux products. *J Atmos Oceanic Technol* 30(6):1072–1090
- Doelling DR, Sun M, Nguyen LT, Nordeen ML, Haney CO, Keyes DF, Mlynchzak PE (2016) Advances in geostationary-derived longwave fluxes for the CERES synoptic (SYN1 deg) product. *J Atmos Oceanic Technol* 33(3):503–521
- Ferek RJ, Garrett T, Hobbs PV, Strader S, Johnson D, Taylor JP, Albrecht BA (2000) Drizzle suppression in ship tracks. *J Atmos Sci* 57(16):2707–2728
- Ghan SJ, Liu X, Easter RC, Zaveri R, Rasch PJ, Yoon JH, Eaton B (2012) Toward a minimal representation of aerosols in climate models: comparative decomposition of aerosol direct, semidirect, and indirect radiative forcing. *J Clim* 25(19):6461–6476
- Giglio L, Randerson JT, van der Werf GR (2013) Analysis of daily, monthly, and annual burned area using the fourth-generation global fire emissions database (GFED4). *J Geophys Res Biogeosci* 118(1):317–328
- Global Modeling and Assimilation Office (GMAO) (2015) MERRA-2 tavgM_2d_int_Nx: 2d, Monthly mean, time-averaged, single-level, assimilation, vertically integrated diagnostics V5.12.4, Greenbelt, MD, USA, Goddard Earth Sciences Data and Information Services Center (GES DISC), Accessed [July 7, 2017] 10.5067/FQPTQ4OJ22TL
- Haywood J, Boucher O (2000) Estimates of the direct and indirect radiative forcing due to tropospheric aerosols: a review. *Rev Geophys* 38(4):513–543
- Haywood JM, Osborne SR, Francis PN, Keil A, Formenti P, Andreae MO, Kaye PH (2003) The mean physical and optical properties of regional haze dominated by biomass burning aerosol measured from the C-130 aircraft during SAFARI 2000. *J Geophys Res Atmos* 108(D13):8473. <https://doi.org/10.1029/2002JD002226>
- Hourdin F, Musat I, Guichard FS, Ruti PM, Favot F, Filiberti MA, Boone A (2010) AMMA-model intercomparison project. *Bull Am Meteorol Soc* 91(1):95–104
- Huang J, Zhang C, Prospero JM (2009a) African aerosol and large-scale precipitation variability over West Africa. *Environ Res Lett* 4(1):015006
- Huang J, Zhang C, Prospero JM (2009b) Large-scale effect of aerosols on precipitation in the West African Monsoon region. *Q J R Meteorol Soc* 135(640):581–594
- Huffman GJ, Bolvin DT, Adler RF (2016) GPCP version 1.2 one-degree daily precipitation data set. Research Data Archive at the National Center for Atmospheric Research, Computational and Information Systems Laboratory, Boulder
- Kaufman YJ, Koren I, Remer LA, Rosenfeld D, Rudich Y (2005) The effect of smoke, dust, and pollution aerosol on shallow cloud development over the Atlantic Ocean. *Proc Natl Acad Sci* 102(32):11207–11212
- Knippertz P, Fink AH, Deroubaix A, Morris E, Tocquer F, Evans MJ, Marsham JH (2017) A meteorological and chemical overview of the DACCIWA field campaign in West Africa in June–July 2016. *Atmos Chem Phys* 17(17):10893–10918
- Koren I, Martins JV, Remer LA, Afargan H (2008) Smoke invigoration versus inhibition of clouds over the Amazon. *Science* 321(5891):946–949

- Kruger AC et al (2010) Strong wind climatic zones in South Africa. *Wind Struct J* 31(1):37–55
- Liu X, Xie X, Yin ZY, Liu C, Gettelman A (2011) A modeling study of the effects of aerosols on clouds and precipitation over East Asia. *Theoret Appl Climatol* 106(3–4):343–354
- Marlon JR, Bartlein PJ, Carcaillet C, Gavin DG, Harrison SP, Higuera PE, Prentice IC (2008) Climate and human influences on global biomass burning over the past two millennia. *Nat Geosci* 1(10):697
- Nicholson SE, Some B, McCollum J, Nelkin E, Klotter D, Berte Y, Noukpozoukounou JN (2003) Validation of TRMM and other rainfall estimates with a high-density gauge dataset for West Africa. Part II: validation of TRMM rainfall products. *J Appl Meteorol* 42(10):1355–1368
- Nwofor OK, Dike VN, Lin Z, Pinker RT, Onyeuwaoma ND (2018) Fine-mode aerosol loading over a sub-sahel location and its relation with the West African monsoon. *Aerosol Sci Eng* 2(2):74–91
- Ramanathan VCPJ, Crutzen PJ, Kiehl JT, Rosenfeld D (2001) Aerosols, climate, and the hydrological cycle. *Science* 294(5549):2119–2124
- Ramanathan V, Chung C, Kim D, Bettge T, Buja L, Kiehl JT, Wild M (2005) Atmospheric brown clouds: impacts on South Asian climate and hydrological cycle. *Proc Natl Acad Sci* 102(15):5326–5333
- Rosenfeld D, Lohmann U, Raga GB, O’dowd DC, Kulmala M, Fuzzi S, Andreae MO (2008) Flood or drought: how do aerosols affect precipitation? *Science* 321(5894):1309–1313
- Shindell DT, Voulgarakis A, Faluvegi G, Milly G (2012) Precipitation response to regional radiative forcing. *Atmos Chem Phys* 12(15):6969–6982
- Stocker TF, Qin D, Plattner GK, Tignor M, Allen SK, Boschung J, Midgley PM (2013) IPCC, 2013: climate change 2013: the physical science basis. Contribution of Working Group I to the Fifth Assessment Report of the Intergovernmental Panel on Climate Change, p 1535
- Tosca MG, Diner DJ, Garay MJ, Kalashnikova OV (2015) Human-caused fires limit convection in tropical Africa: first temporal observations and attribution. *Geophys Res Lett* 42(15):6492–6501
- Twomey S, Gall R, Leuthold M (1987) Pollution and cloud reflectance. *Bound-Layer Meteorol* 41(1–4):335–348
- Van Der Werf GR et al (2017) Global fire emissions estimates during 1997–2016. *Earth Syst Sci Data* 9:697–720
- Wilcox EM (2012) Direct and semi-direct radiative forcing of smoke aerosols over clouds. *Atmos Chem Phys* 12(1):139–149
- Wilcox EM, Thomas RM, Praveen PS, Pistone K, Bender FAM, Ramanathan V (2016) Black carbon solar absorption suppresses turbulence in the atmospheric boundary layer. *Proc Natl Acad Sci* 113(42):11794–11799
- Wild M (2012) Enlightening global dimming and brightening. *Bull Am Meteorol Soc* 93(1):27–37
- Xie X, Wang H, Liu X, Li J, Wang Z, Liu Y (2016) Distinct effects of anthropogenic aerosols on the East Asian summer monsoon between multidecadal strong and weak monsoon stages. *J Geophys Res Atmos* 121(12):7026–7040
- Zhang Y, Fu R, Yu H, Qian Y, Dickinson R, Silva Dias MAF, da Silva Dias PL, Fernandes K (2009) Impact of biomass burning aerosol on the monsoon circulation transition over Amazonia. *Geophys Res Lett* 36:L10814. <https://doi.org/10.1029/2009GL037180>
- Zuidema P, Redemann J, Haywood J, Wood R, Piketh S, Hipondoka M, Formenti P (2016) Smoke and clouds above the southeast Atlantic: upcoming field campaigns probe absorbing aerosol’s impact on climate. *Bull Am Meteorol Soc* 97(7):1131–1135

Publisher’s Note Springer Nature remains neutral with regard to jurisdictional claims in published maps and institutional affiliations.